RESEARCH

Evaluation of prevention and treatment effects of fibroblast growth factor-21 in BLM-induced pulmonary fibrosis

Xiangxiang Wang[1,2] · Shuang Li[1] · Jinmiao Liu[1] · Wenying Sun[1] · Han Zhao[1] · Qing Han[1] · Yijia Liu[1] · Xiaolin Cao[1] · Qianhui Li[1] · Yuhan Jin[1] · Xiaochen Guo[1] · Guiping Ren[1,3,4]

Abstract

Pulmonary fibrosis is a progressive and fatal fibrotic lung disease and associated with a high mortality rate. In the study, the prevention and treatment effects of fibroblast growth factor-21 (FGF-21) in bleomycin (BLM)-induced pulmonary fibrosis were investigated in vivo and vitro. In the prevention of pulmonary fibrosis studies, the results showed that interdict of FGF-21 could reduce the related gene and protein expression levels of pulmonary fibrosis. In addition, FGF-21 significantly reduced both the aggregation of inflammatory cells and deposition of collagen in the lung by histopathology. In therapy of pulmonary fibrosis studies, the results indicated that treatment with FGF-21 resulted in an amelioration of the pulmonary fibrosis in mice with reductions of the pathological score, collagen deposition and transforming growth factor (TGF)-β and α-smooth muscle actin (α-SMA) expressions in the lung tissues at fibrotic stage, and late administration was also able to reduce the degree of pulmonary fibrosis and even better than these in the prevention group. Furthermore, BLM-induced THP-1 macrophage model was verified using FGF-21; the result showed that FGF-21 decreased the related gene expression level of pulmonary fibrosis. FGF-21 may have preventive and therapeutic effects on BLM-induced pulmonary fibrosis via inhibiting myofibroblast differentiation and inflammatory. Thus, FGF-21 represents a potential drug for the prevention and treatment of pulmonary fibrosis.

Keywords Pulmonary fibrosis · Fibroblast growth factor-21 · TGF-β · α-SMA · Inflammatory response

Introduction

Pulmonary fibrosis is a chronic, progressive, and lethal pulmonary disease, and it is the most common phenomenon of the interstitial pneumonia. The etiology of pulmonary fibrosis is characterized with excessive fibroblast proliferation and extracellular matrix (ECM) remodeling resulting in deteriorating lung function (Phan et al. 2021). The incidence and prevalence of pulmonary fibrosis continue rising, and the median time to death from diagnosis is only 3 to 5 years which is worse than that of many cancers. It had also a sequela in severe patients with the coronavirus disease 2019 (COVID-19) (Kalluri et al. 2020; Zhang et al. 2021).

The pathogenesis of pulmonary fibrosis is mainly caused by excessive myofibroblast accumulation in fibroblastic foci which distorted pulmonary structure. Myofibroblasts could arrive from the differentiation of resident fibroblast, recruitment of circulating fibrocytes, and transition of epithelial mesenchymal cell (Yang et al. 2019). Therefore, fibroblasts are important effector cells to differentiate into myofibroblasts and overproduce ECM in pulmonary fibrosis, while myofibroblasts are distinguished by the collagen deposition and α-smooth muscle actin (α-SMA) expression (Tao et al. 2017). Collagen type I and type III are the main collagen components involved in pulmonary fibrosis. And α-SMA is regarded as the marker of fibroblasts differentiate into myofibroblasts (Yang et al. 2019). Transforming growth factor (TGF)-β is a crucial profibrotic factor in pulmonary fibrosis and plays an important role in

✉ Xiaochen Guo
676553202@qq.com

✉ Guiping Ren
renguiping@126.com

1   Biopharmaceutical Lab, College of Life Science, Northeast Agricultural University, 600 Changjiang Road, Harbin 150030, China

2   Institute of Microbiology, Heilongjiang Academy of Sciences, Harbin 150010, China

3   Research Center of Genetic Engineering of Pharmaceuticals of Heilongjiang Province, Northeast Agricultural University, Harbin 150030, China

4   Key Laboratory of Agricultural Biological Functional Gene, Northeast Agricultural University, Harbin 150030, China

induction of epithelial-to-mesenchymal transition, inflammatory response, myofibroblast differentiation, and ECM molecule accumulation of pulmonary fibrosis, which has a high expression level in lung fibrosis in patients (Goodwin and Jenkins 2009). And it is involved in many fibrogenic pathways, including myofibroblast differentiation, collagen synthesis and deposition (Kang 2017). Previous studies have indicated that fibroblast growth factor-21 (FGF-21) is a cytokine mainly secreted by the liver and plays a variety of biological functions such as regulating lipid and sugar metabolism, anti-oxidative, and anti-inflammatory effects (Xie and Leung 2017). Recent studies showed that FGF-21 could inhibit inflammatory response and oxidative stress in the body which was closed relation to the development of pulmonary fibrosis (Kseibati et al. 2020). In addition, it was reported that FGF-21 attenuated hepatic fibrogenesis and high glucose-induced fibrogenesis in mesangial cells (Li et al. 2017; Xu et al. 2016). Pirfenidone is an oral anti-fibrotic and anti-inflammatory agent that was used for the treatment of pulmonary fibrosis (Cao et al. 2022; Pourgholamhossein et al. 2018). Due to the similar anti-fibrotic and anti-inflammatory effect of pirfenidone and FGF-21, therefore we hypothesized that FGF-21 could be antifibrotic and protect against bleomycin (BLM)-induced pulmonary fibrosis, and the prevention and treatment effects of FGF-21 was evaluated in BLM-induced pulmonary fibrosis in mouse model and cell model.

Materials and methods

Protein and reagents

Recombinant FGF-21 protein was produced by the Biopharmaceutical Laboratory of Northeast Agricultural University. TRIzol® reagents (CAS: 9108) were obtained from Takara, Japan. Fetal bovine serum (FBS, CAS: 10,099–141) and RMPI-1640 (CAS: C11875500BT) were purchased from Gibco, USA. Phorbol-12-myristate13-acetate (PMA, CAS: 16,561–29-8) was purchased from Sigma, USA.

Mouse model of BLM-induced pulmonary fibrosis

One hundred and twenty 8-week-old male C57BL/6 (SPF) were purchased from the Experimental Animal Center of Changchun YiSi Company. The mice were acclimated and housed individually in standardized cages with enough nesting material-sawdust in a temperature and humidity-controlled pathogen-free room (temperature: 24 ± 1 °C; relative humidity: $50 \pm 5\%$), on a 12-h light cycle with free access to food and water. After 1 week of pre-feeding, these mice were randomly divided into 6 groups, including normal control group (normal), model control group (PBS), low-dose

FGF-21 prevention group (FL), medium-dose FGF-21 prevention group (FM), high-dose FGF-21 prevention group (FH), and high-dose FGF-21 treatment group (FT). To induce pulmonary fibrosis, the mice were administered intratracheally with BLM in 50 μL of saline at a dose of 3 mg/kg under nembutal anesthesia. The mice were received intratracheally with 50 μL of saline in the same way in normal group. In prevention of pulmonary fibrosis studies, the mice were administered with the low-dose, medium-dose and high-dose of FGF21 (1, 5, and 10 mg/kg) by intraperitoneal injection after intratracheal instillation, respectively. In therapy of pulmonary fibrosis studies, the mice were administered with FGF21 at a dose of 10 mg/kg by intraperitoneal injection on 7 days after received BLM. The mice were administered with PBS by intraperitoneal injection in PBS group. Five mice were euthanized on 7, 14, 21, and 28 days after injection of FGF21, and the lungs were collected for histopathology, immunohistochemistry, real-time PCR, collagen assay, and western blot analysis.

Lung fibrosis and Ashcroft Score

Lung tissue was fixed in 4% paraformaldehyde, embedded in paraffin and cut into 5-μm sections. The sections were stained with H&E or Masson's trichrome (CAS: G1340, Solarbio, China) and estimated the score (0–8 scale) of fibrosis severity using the grading system described by Ashcroft et al. (1988). Collagen content in the lung tissue was determined using Hydroxyproline Detection Kit (CAS: A030-2, Nanjing Jiancheng Bioengineering Institute, China).

Immunohistochemistry

The sections of lung tissue were processed with antigen retrieval in 0.01 mol/L citrate buffer (pH = 6.0) and then placed in 3% H_2O_2. The sections were incubated with rabbit anti-α-SMA antibody (1:100, CAT: ab5694, Abcam, USA) or rabbit anti-TGF-β1 antibody (1:100, CAT: ab92486, Abcam, USA) at 37 °C for 1 h, followed using the HRP-labeled goat anti-rabbit secondary antibody (1:200, CAT: ab6721, Abcam, USA). The reaction was visualized with DAB solution (CAT: P0203, Beyotime, China). After counterstaining with hematoxylin, the sections were captured with an inverted microscope (Olympus, Japan) and analyzed using ImageJ analysis software.

Real-time PCR analysis

Total RNA was isolated using Trizol reagent and reverse-transcribed into cDNA using M-MLV reverse transcriptase (CAT: M1705, Promega, USA). Itaq SYBR Green Supermix was used for real-time PCR with a Bio-Rad Hercules CA machine. Primers for α-SMA, COL-1, COL-3, TNF-α,
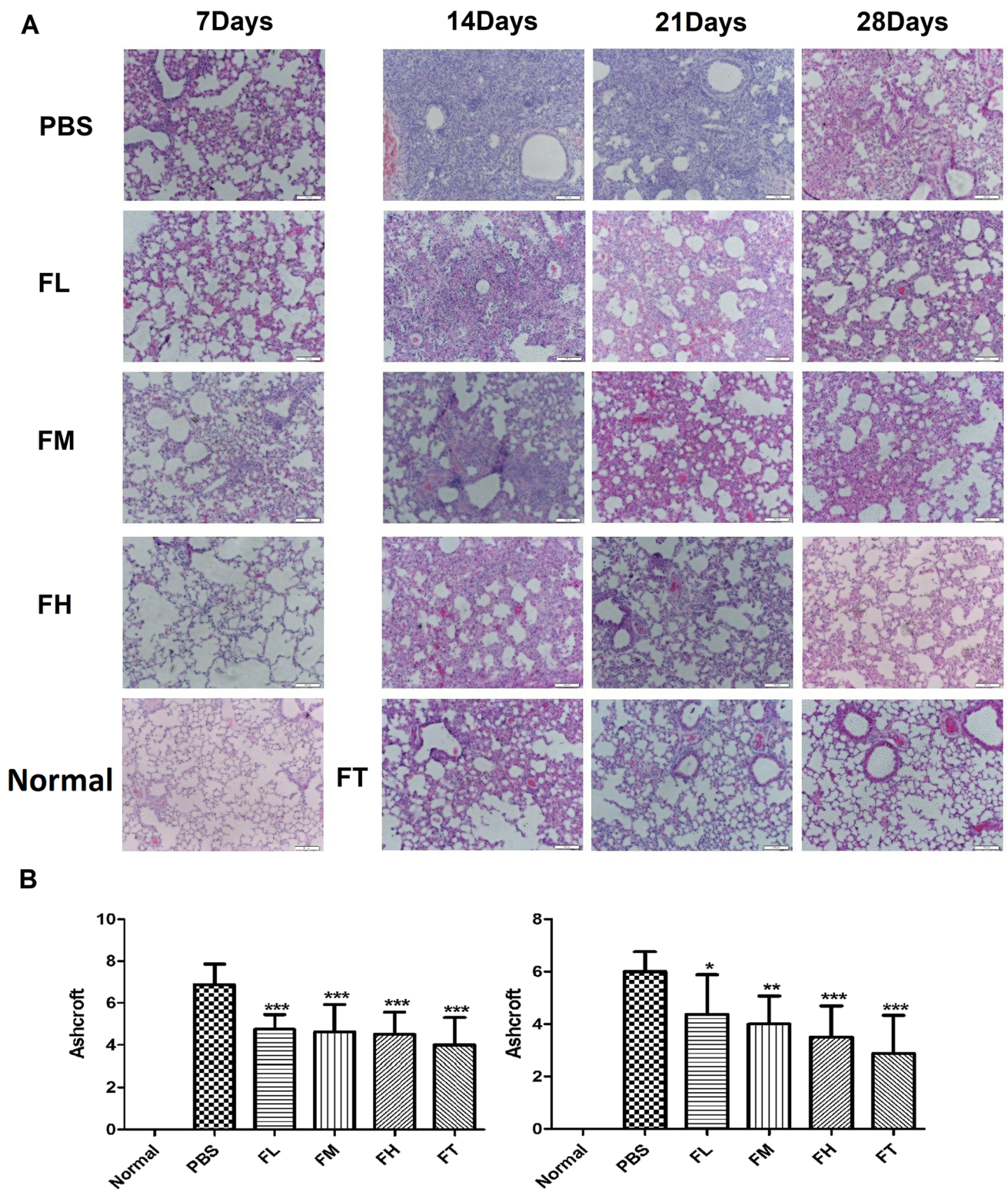
Fig. 1 Morphopathological change in the lung tissues of mice. **A** The histopathological of lungs in mice were measured by H&E staining at 7, 14, 21, and 28 days after molding. **B** Quantitative assessment of H&E staining at 14 and 28 days after molding was performed using the Ashcroft score ($n=3$), respectively. Data were expressed as the means $\pm$ SD. $*p<0.05$, $**p<0.01$, $***p<0.001$ vs the PBS group; bar$=100$ μm
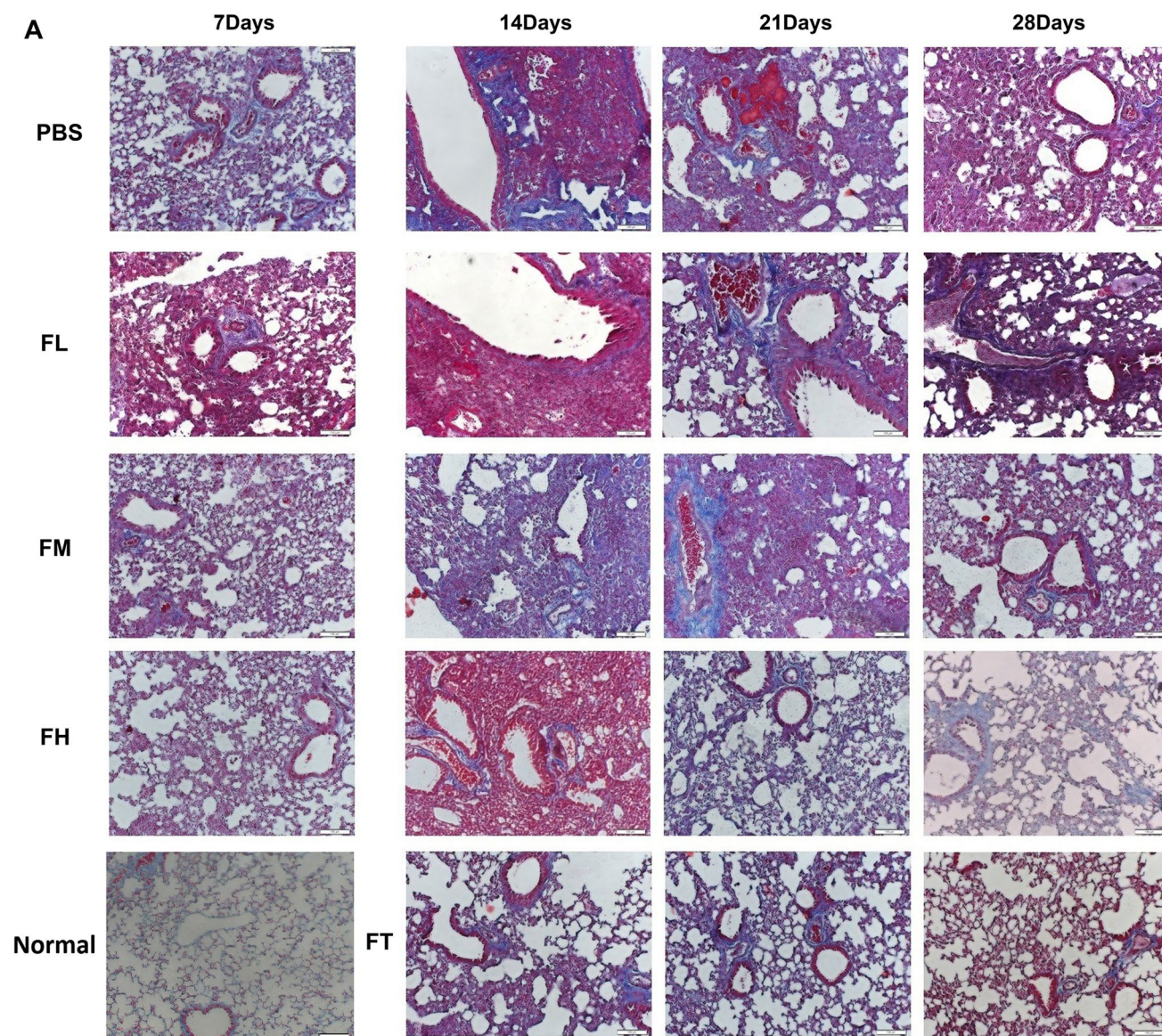
A

Fig. 2 The collagen change in the lung tissues of mice. **A** Detection of the collagen change by Masson's trichrome staining at 7, 14, 21, and 28 days after molding. **B** Quantitative assess the collagen content of Masson's trichrome staining at 14 and 28 days after molding ($n = 3$), respectively. **C** Measurement of the mRNA expression level of Col-1 and Col-3 by real-time PCR at 14 and 28 days after molding. **D** Detection of hydroxyproline levels by Hydroxyproline Detection Kit. Data were expressed as the means $\pm$ SD. $*p < 0.05$, $**p < 0.01$, $***p < 0.001$ vs the PBS group; bar $= 100$ μm

TGF-β, IL-1β, and β-actin were shown as follows: mα-SMA forward: CCGAGATCTCAC CGAC reverse: TCCAGA GCTACATGACACAG; mCol-1 forward: GACTGGAAG AGCGGAG AGTACTG reverse: CCTTGATGGCGTCCA GGTT; mCol-3 forward: CTGTAACATGGAAAC TGG GGAAA reverse: CCATAGCTGAACTGAAAACCACC; mTNF-α forward: CCCTCACAC TCAGATCATCTTCT reverse: GCTACGACGTGGGCTACAG; mTGF-β forward: ATGCTAAA GAGGTCACCCGC reverse: TGCTTCCCG AATGTCTGACG; mIL-1β forward: GCAACTGTT CCT GAACTCAACT reverse: ATCTTTTGGGGTCCGTCA ACT; mβ-klotho forward: ACATCT GCTGGAAGGTGG AC reverse: GGTACCACCATGTACCCAGG; hα-SMA forward: TTCCAG CCATCCTTCATC reverse: ATTGTT AGCATAGAGGTCCTT; hCol-1 forward: GTGCGATGA CGTGATCTGTGA reverse: CGGTGGTTTCTTGGTCGG T; hCol-3 forward: GCCAAATATGT GTCTGTGACTCA reverse: GGGCGAGTAGGAGCAGTTG; hTNF-α forward: GAGGCCAAG CCCTGGTATG reverse: CGGGCC GATTGATCTCAGC; hTGF-β forward: CTAATGGTGGA AACCCACAACG reverse: TATCGCCAGGAATTGTTG CTG; hIL-8 forward: ACTGAGAGTG ATTGAGAGTGGA
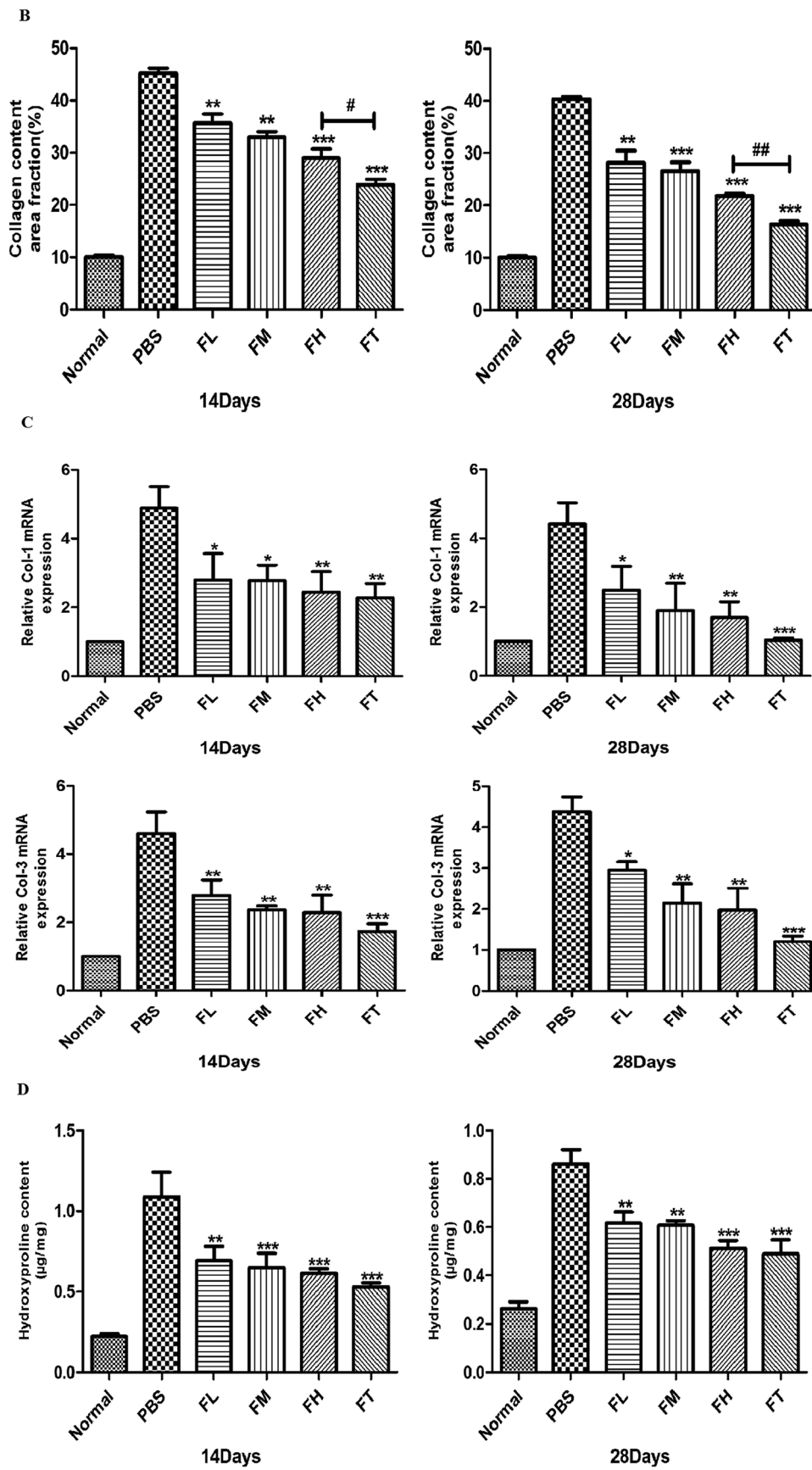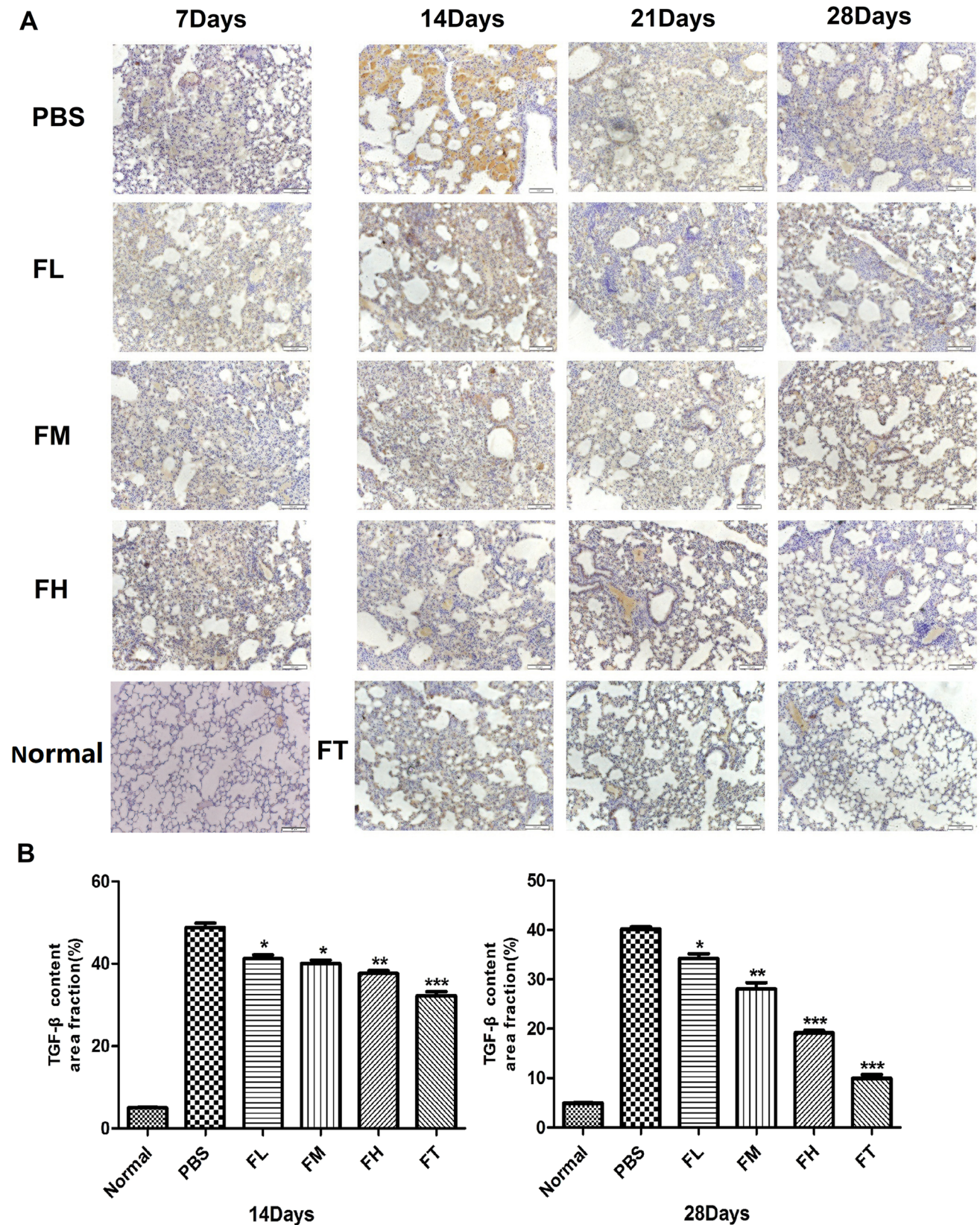
Fig. 2 (continued)

Fig. 3 Measurement of the expression level of TGF-β in the lung tissues of mice. **A** Detection of the expression level of TGF-β by immunohistochemical staining ($n=6$) at 14 and 28 days after molding. **B** Quantitative assess the TGF-β content of immunohistochemical staining at 14 and 28 days after molding. **C** Detection of the mRNA expression level of TGF-β by real-time PCR. **D** Measurement of the protein expression level of TGF-β by western blot ($n=3$). Data were expressed as the means±SD. *$p<0.05$, **$p<0.01$, ***$p<0.001$ vs the PBS group; bar=100 μm
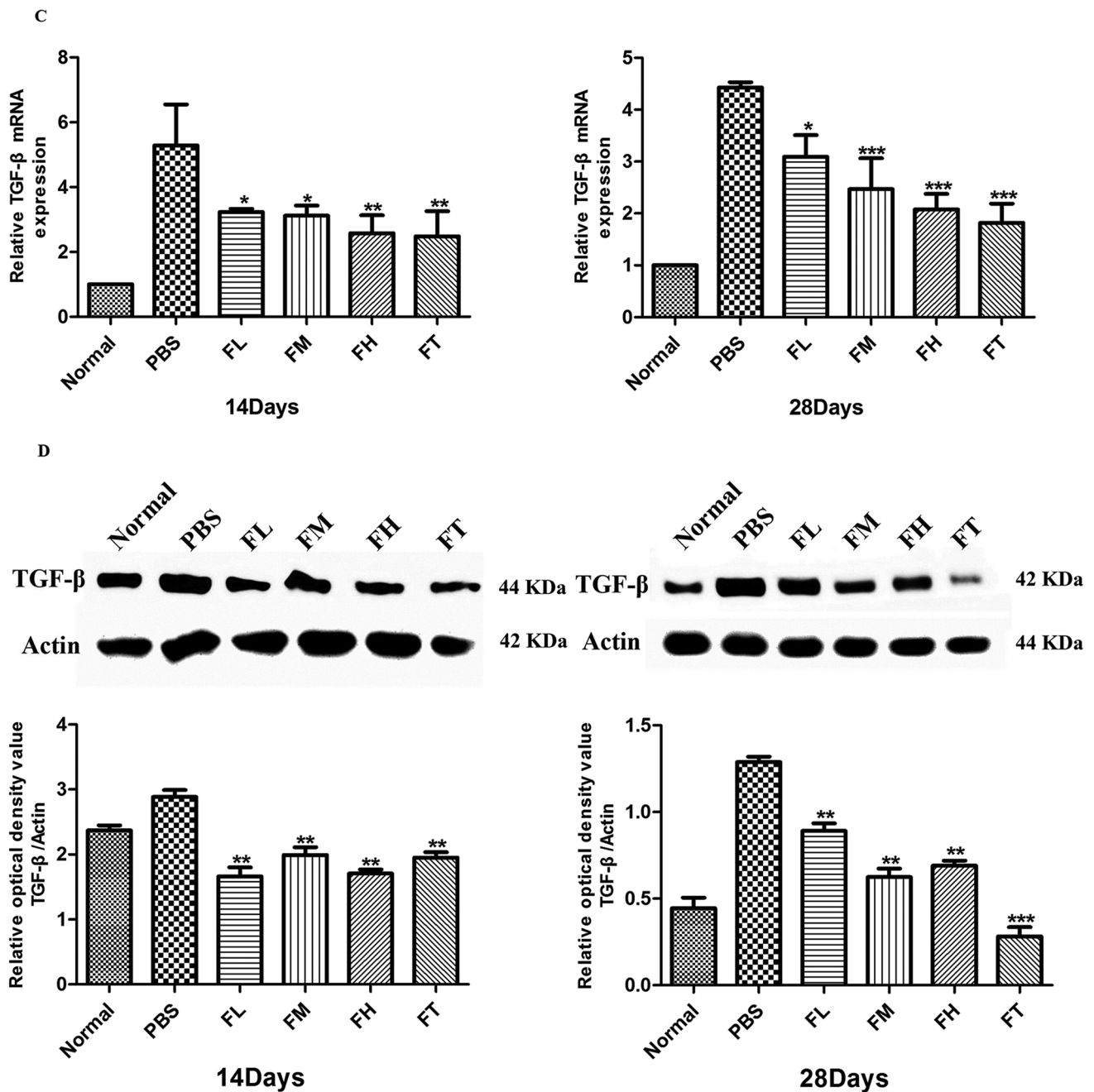
C

D

Fig. 3 (continued)

C reverse: AACCCTCTGCACCCAGTTTTC; hβ-klotho forward: CATGTA CGTTGCTATCCAGGC reverse: CTCCTT AATGTCACGCACGAT.

Western blot

The lung tissue or THP-1 macrophages were lysed for total protein extraction in RIPA buffer (CAT: W062-1–1, Nanjing Jiancheng Bioengineering Institute, China)

following the manufacturer's protocols. The protein concentration was measured using the BCA protein Assay Kit (CAT: P0010S, Beyotime, China). These protein samples were separated using SDS-PAGE and transferred onto nitrocellulose membranes. The membrane was blocked with the 5% skim milk in PBS at 37 °C for 2 h. The membrane was then incubated with the primary antibody against TGF-β (1:1000, CAT: ab92486, Abcam, USA), α-SMA (1:1000, CAT: ab5694, Abcam, USA), or β-actin
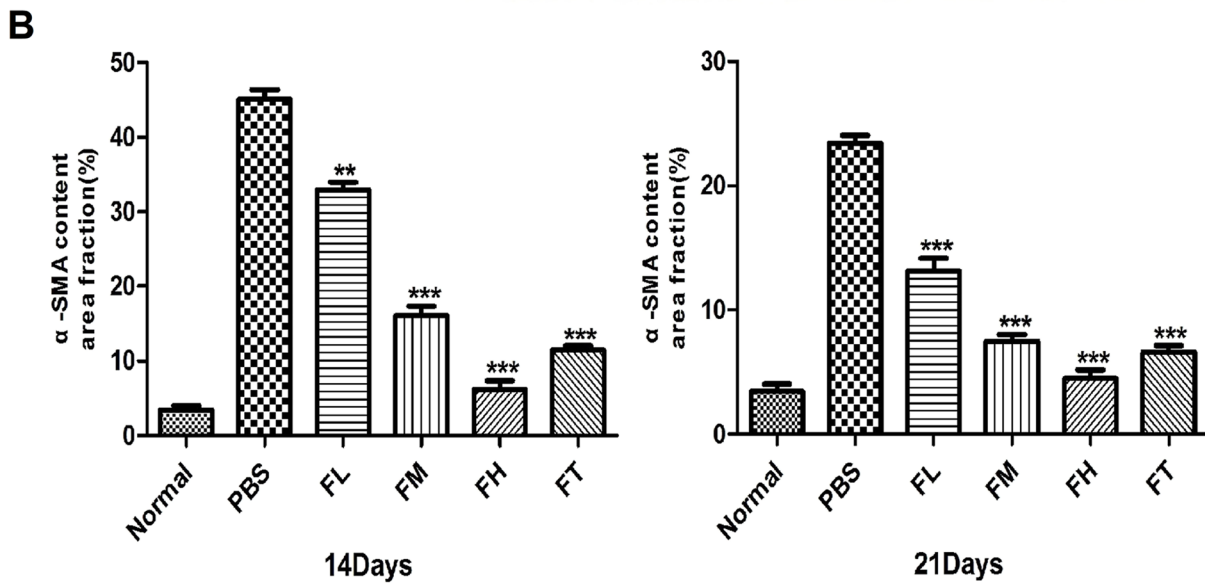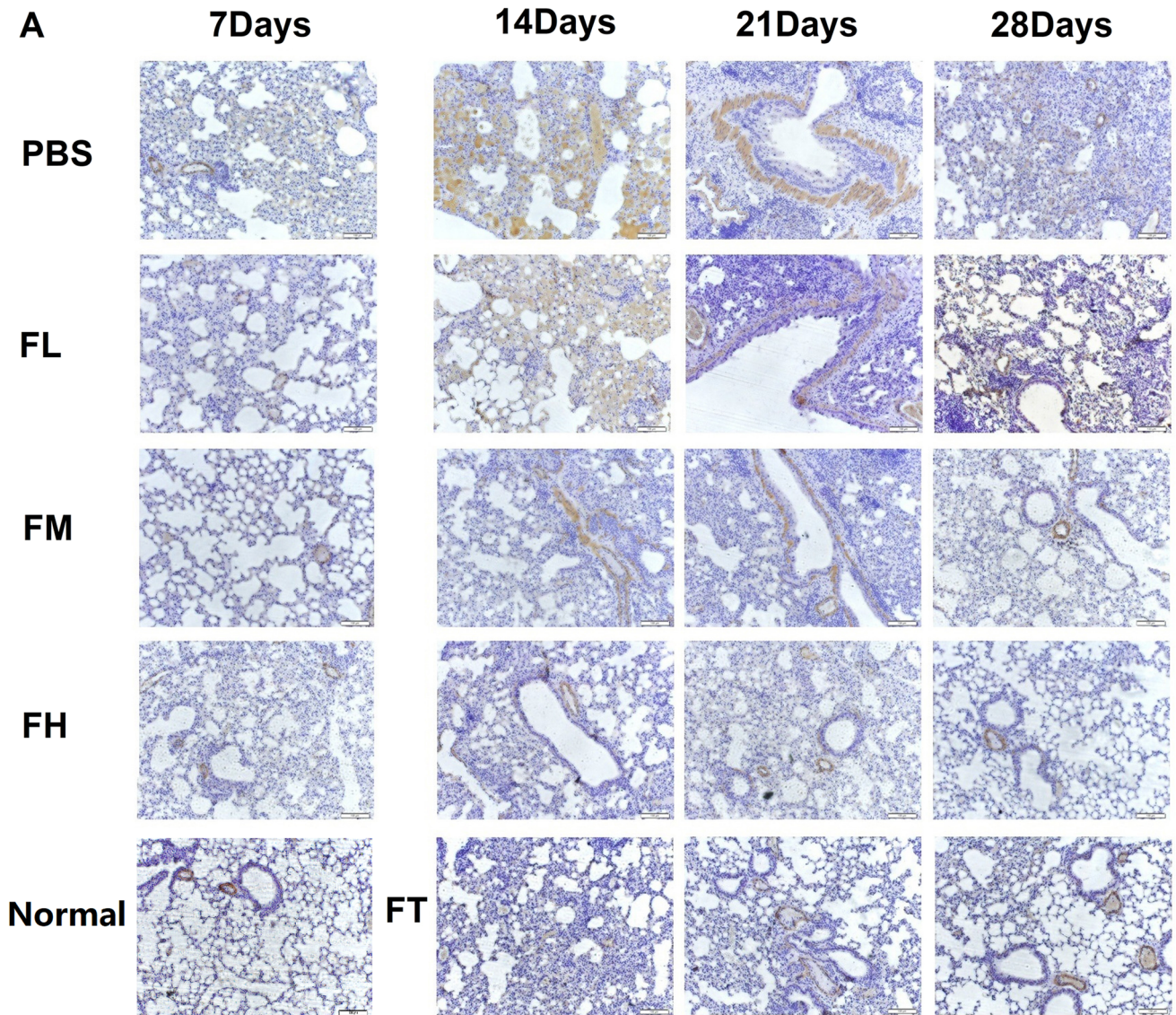
◀ **Fig. 4** Detection of the expression level of α-SMA in the lung tissues of mice. **A** Measurement of the expression level of α-SMA by immuno-histochemical staining (*n*=6) at 7, 14, 21, and 28 days after molding. **B** Quantitative assess the α-SMA content of immunohistochemical staining at 14 and 21 days. **C** Detection of the mRNA expression level of α-SMA by real-time PCR. **D** Measurement of the protein expression level of α-SMA by western blot (*n*=3). Data were expressed as the means±SD. *$p<0.05$, **$p<0.01$, ***$p<0.001$ vs the PBS group; bar=100 μm

(1:1000, CAT: 8H10D10, CST, USA) overnight at 4 ℃. The membrane was then incubated with HRP-conjugated rabbit or mouse IgG (1:7500) as secondary antibody at 37 ℃ for 1 h. The finalized membrane was detected screened by an ECL detection system. β-actin was used as the loading control.

Cell culture and treatment

The human monocytic THP-1 cells were cultured in RMPI-1640 containing 10% FBS in a 6-well plate and incubated with 100 ng/mL PMA for 3 days to differentiate into macrophages. Then, the THP-1 macrophages were treated with BLM with 50 mU/mL of the RPMI-1640 with 10% FBS for 6, 12, 24, and 48 h with or without FGF-21 (high dose: 1 mM) for real-time PCR and Western blotting analysis.
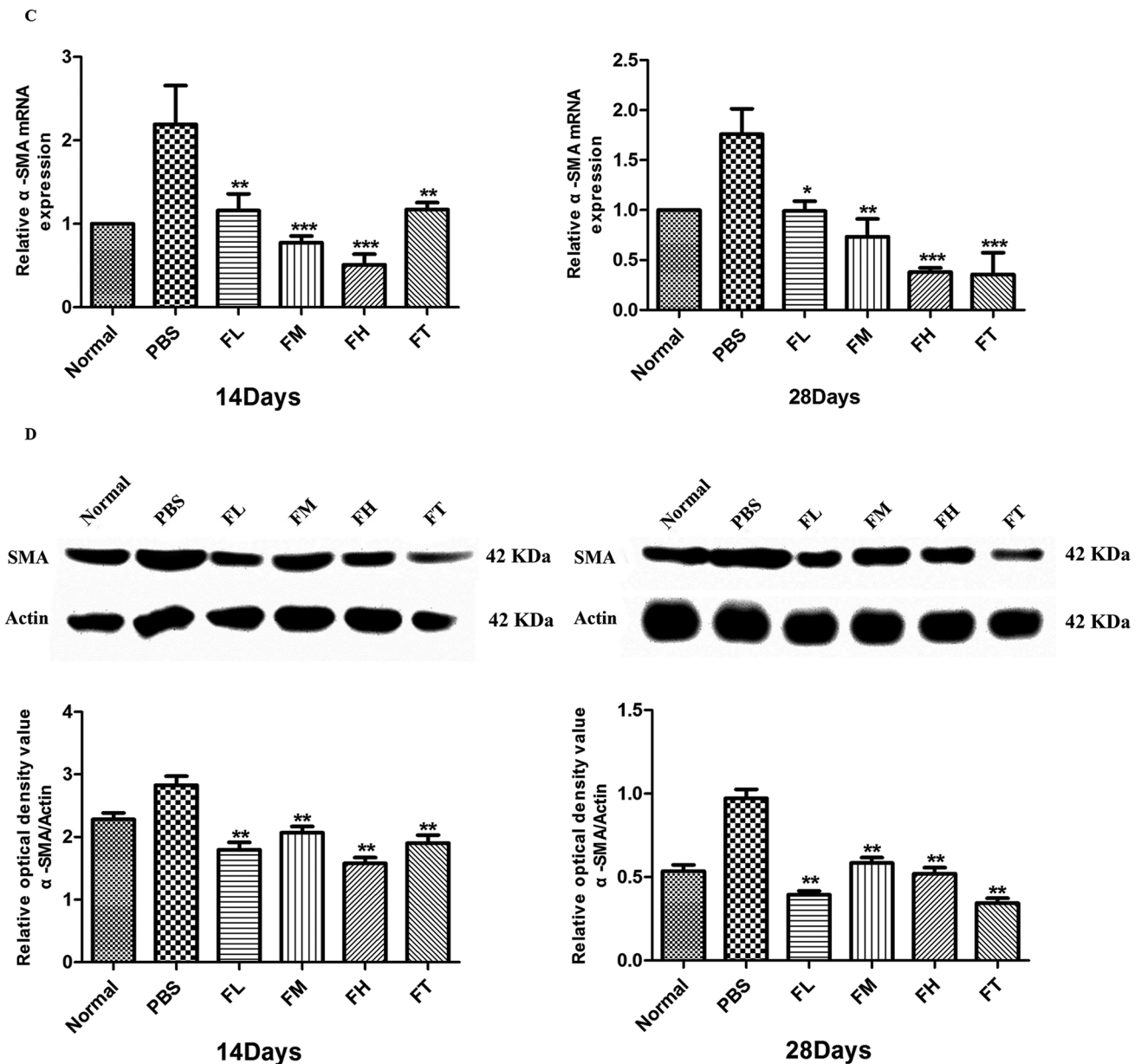

Fig. 4 (continued)

Fig. 5 Therapeutic effect of FGF-21 in THP-1 macrophages model. **A** Detection of the expression level of TGF-β, α-SMA, Col-1, Col-3, IL-8, and TNF-α in THP-1 macrophages at 6, 12, 24, and 48 h after molding. **B** Measurement of the mRNA expression level of TGF-β, α-SMA, Col-1, Col-3, IL-8, and TNF-α by real-time PCR. **C** Detection of the expression level of TGF-β and α-SMA by western blot. Data were expressed as the means ± SD. *$p < 0.05$, **$p < 0.01$, ***$p < 0.001$ vs the BLM group; bar = 100 μm
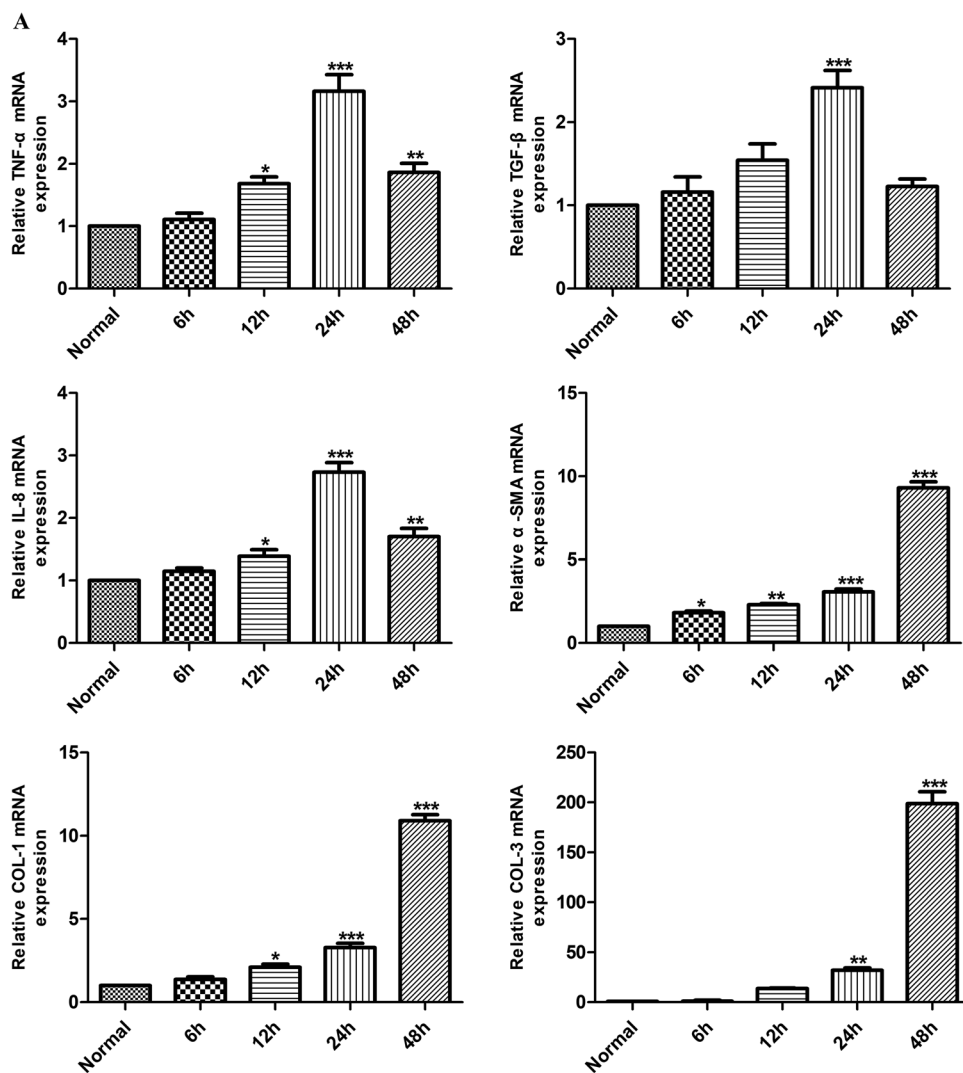
Statistical analysis

All data were presented as the mean ± SEM. Significance ($p < 0.05$) of the differences were assessed by one-way ANOVA on GraphPad Prism 5.0 software. A *P*-value of less than 0.05 was considered to be statistically significant.

Results

Effect of FGF21 on the morphopathological and collagen changes in mice

The BLM-induced animal model is a useful tool to investigate treatment options for pulmonary fibrosis. The effect of FGF21 on pulmonary inflammation and collagen fibers was examined by H&E staining, Masson's trichrome staining, real-time PCR, and the hydroxyproline (HYP)

analysis in mice with BLM-induced pulmonary fibrosis. H&E staining and Masson's trichrome staining were used to assess the typical morphopathological changes in the lung tissue. The results of H&E staining showed that the fibrogenic response started at 7 days and achieved to the peak at 14 days after BLM intratracheal instillation (molding), and severe distortion of structure and large fibrous areas were placed in the total lung tissue in PBS group. Mice in prevention groups received FGF21 at 0 day after molding and which in treatment group received FGF21 at 7 days after molding. The result demonstrated that FGF21 significantly reduced the infiltration of inflammatory cells and the severity of pulmonary fibrosis around the airways in prevention and treatment groups (Fig. 1A). FGF21 also reduced fibrosis in the lung parenchyma as quantified with the Ashcroft grading system using a predetermined 0 to 8 scale of severity. Interestingly, the results showed that FGF21 significantly reduced the severity of

Fig. 5 (continued)
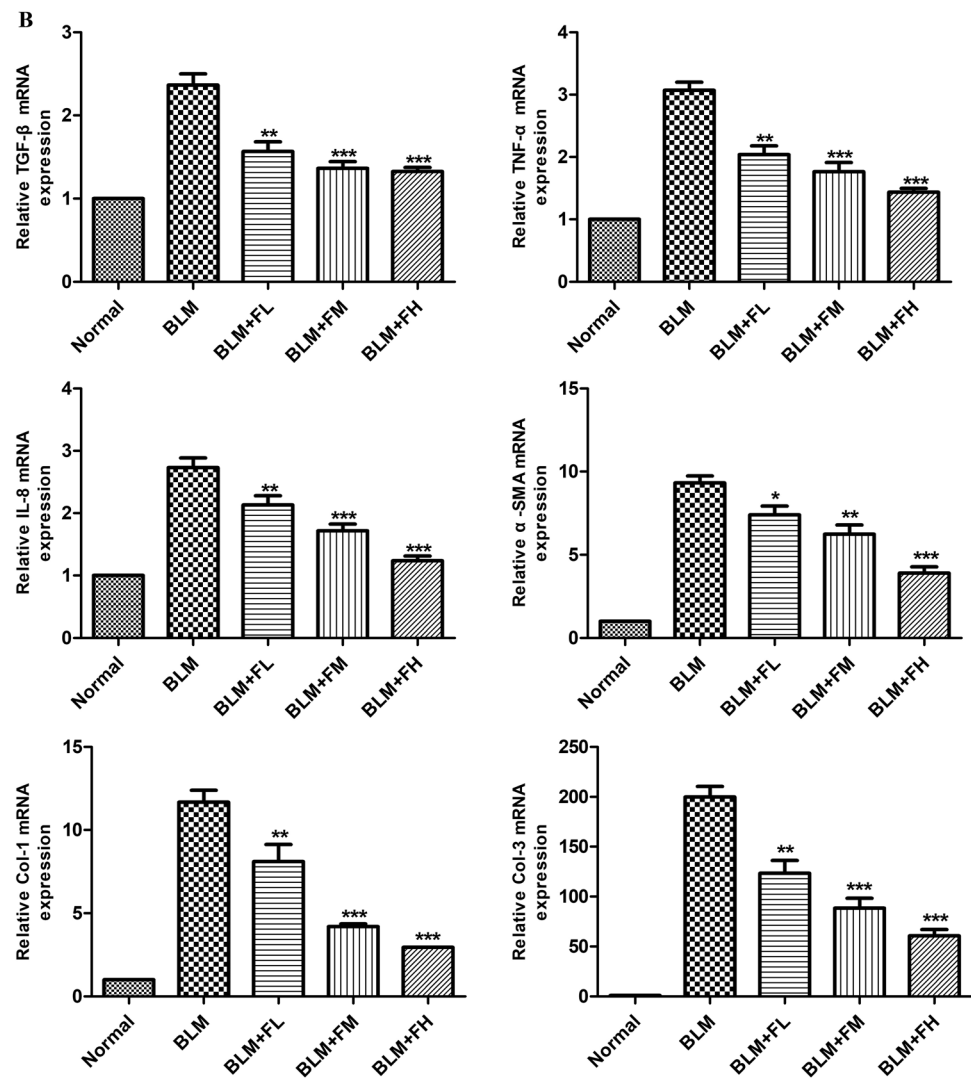
fibrosis around the airways and the total lung at 14 and 28 days after molding in prevention and treatment groups (***$p < 0.001$ or **$p < 0.01$ or *$p < 0.05$), and the prevention effect of FGF21 in mice was in a dose dependent in prevention groups, and the treatment effect of FGF21 in mice was better than its prevention effect. (Fig. 1B). The result of Masson's staining showed that the collagen seriously deposed around trachea and vessels of the lungs of mice at 14 days after molding in PBS group; after mice were injected FGF-21 in prevention groups, collagen deposition obviously reduced at 14 and 28 days after molding and it was in dose dependent (***$p < 0.001$ or **$p < 0.01$ or *$p < 0.05$). And the collagen of pulmonary interstitial and around trachea of lungs of mice in treatment group significantly reduced compared with that in PBS group at 14 and 28 days after molding, while the lung structure was similar to the normal lung at 28 days after molding in treatment group (***$p < 0.001$ or **$p < 0.01$) (Fig. 2A, B).

Furthermore, the collagen content was detected by real-time PCR and the HYP analysis. The results demonstrated that BLM-induced mice significantly increased the mRNA expression level of Col-1 and Col-3 in the lungs by real-time PCR and the HYP content of the lungs compared with those in normal group, which indicated that BLM stimulated collagen synthesis. The mRNA expression level of Col-1 and Col-3 and the HYP content in the lungs observably reduced in prevention and treatment group, and the therapy effect of mice in treatment group was better than those in prevention groups at 14 days and 28 days after molding (***$p < 0.001$ or **$p < 0.01$ or *$p < 0.05$) (Fig. 2C, D). These results clearly implied that FGF-21 ameliorated and reversed BLM-induced pulmonary fibrosis by directly inhibiting the pulmonary extracellular matrix deposition in prevention and treatment groups, while the therapy effect of mice in treatment group was superior to that in prevention groups.

Fig. 5 (continued)
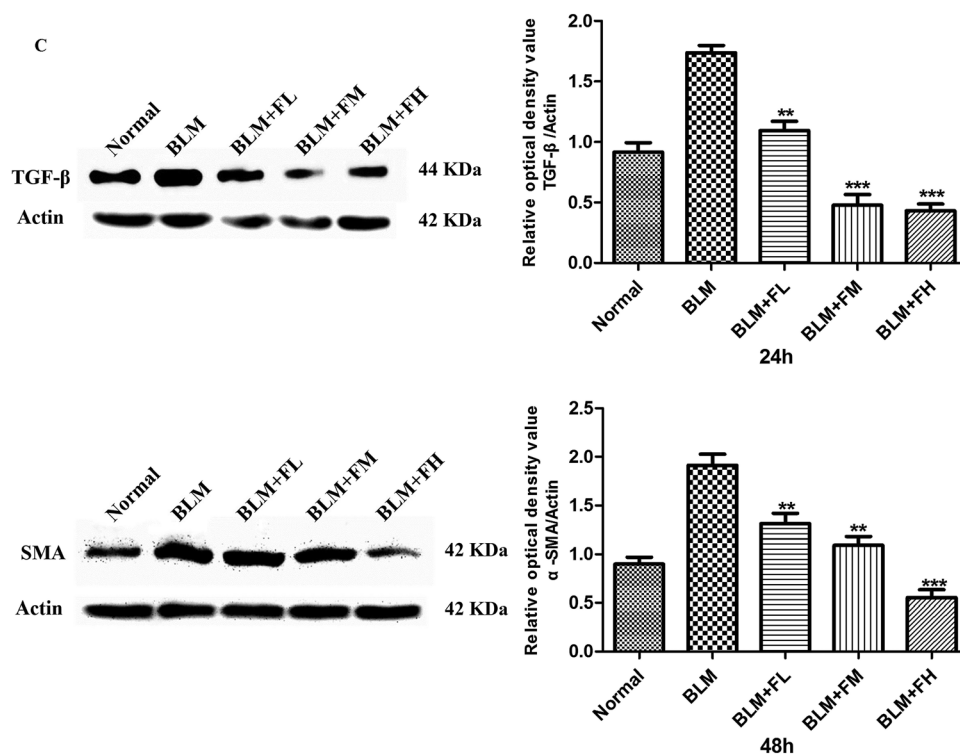
FGF-21 regulated the expression of TGF-β on the established BLM-induced pulmonary fibrosis in mice

TGF-β is a vital profibrotic cytokine that mediates the development of BLM-induced pulmonary fibrosis. Thus, the expression level of TGF-β was investigated in the lung tissue by the immunohistochemical examination. The results showed that TGF-β was restricted to the vessel walls and the interstitium of lung in mice, and the expression level of TGF-β dramatically increased at 14 days and slightly decreased at 28 days after molding in PBS group. The expression level of TGF-β in the lung of mice reduced at 14 and 28 days after molding in prevention and treatment groups, and the effect of FGF21 was in a dose-dependent manner in prevention groups (***$p < 0.001$ or **$p < 0.01$ or *$p < 0.05$). Especially, the expression level of TGF-β was not obviously visible in mice at 28 days after molding in the FM and FH groups (Fig. 3A, B). Furthermore, the expression level of TGF-β was measured by real-time PCR and western blot analysis. The results also revealed that the expression level of TGF-β of lung in mice significantly upregulated in PBS group compared with that in normal group and which observably reduced at 14 and 28 days after molding in prevention and treatment groups (***$p < 0.001$ or **$p < 0.01$ or *$p < 0.05$). The mRNA expression level of TGF-β of lung in mice in FT group was the lowest than that in other groups at 14 and 28 days after molding, and the protein expression level of which

in FT group was the lowest than that in other groups at 28 days after molding (Fig. 3C, D). The results indicated that the alleviation of FGF-21 in BLM-induced pulmonary fibrosis was associated with the expression level of TGF-β. As seen by immunohistochemistry, real-time PCR, and western blot, FGF-21 significantly reduced fibrosis in the lung parenchyma, and even the treatment effect was better than the prevention effect.

FGF-21 regulated the expression of α-SMA on the established BLM-induced pulmonary fibrosis in mice

α-SMA has been suggested to be a specific marker of myofibroblasts; it may convert fibroblasts into myofibroblasts that secrete a large amount of ECM to further aggravate pulmonary fibrosis. The expression level of α-SMA in the lungs of mice was detected by immunohistochemical. The result demonstrated that the expression level of α-SMA increased in the interstitium of lungs of mice at 14 days, and α-SMA staining is widely expressed around the trachea of lung in mice at 21 days after modeling in PBS group, which significantly reduced at 14 and 28 days after molding in prevention and treatment groups; especially, it reduced or even disappeared at 28 days after molding in FH group, and the effect of FGF21 was in a dose-dependent manner in prevention groups (***$p < 0.001$ or **$p < 0.01$) (Fig. 4A, B). Furthermore, the expression level of α-SMA of the lung in mice was identified by real-time PCR and western blot

analysis. The result showed that the mRNA expression level of α-SMA of the lung in mice observably reduced at 14 and 28 days after molding in prevention and treatment groups (***p < 0.001 or **p < 0.01 or *p < 0.05), and in the FH group, it was the lowest than that in other groups at 14 days after molding, while in FH and FT groups, it was similar and lower than that in other groups at 28 days after molding (Fig. 4C). The protein expression level of α-SMA significantly reduced at 14 and 28 days after molding in prevention and treatment groups (***p < 0.001 or **p < 0.01), and in the FH group, it was the lowest than that in other groups at 14 days after molding, while in the FT group, it was the lowest than that in other groups at 28 days after molding (Fig. 4D). These results indicated that FGF-21 inhibited the expression of α-SMA in mice with BLM-induced pulmonary fibrosis, and the treatment effect was better than the prevention effect in the late stage of pulmonary fibrosis.

FGF-21 inhibited inflammation in BLM-induced pulmonary fibrosis in cell models

To further verify the effect of FGF-21 in alleviating pulmonary fibrosis, the cell model was established with BLM in THP-1 macrophages. The results showed that the mRNA expression level of inflammatory cytokines reached the peak at 24 h after molding, and that of collagen genes reached the peak at 48 h after molding. Compared with the THP-1 macrophages in normal group, the mRNA expression levels of α-SMA, Col-1, and Col-3 were 9.5, 10.5, and 198.5-fold higher than those at 48 h, and those of IL-8, TGF-β, and TNF-α were the highest at 24 h after molding in BLM group (Fig. 5A). The result showed that the mRNA expression levels of inflammatory cytokines and collagen genes dramatically reduced, and it was dose dependent at 48 h after molding in THP-1 macrophages in FGF21 groups (Fig. 5B). The result showed that the protein expression level of TGF-β significantly reduced, and it was in a dose dependent at 24 h after molding in THP-1 macrophages in FGF21 groups, while that of α-SMA dramatically reduced in FGF21 groups and was the lowest in FH group at 48 h after molding in THP-1 macrophages (Fig. 5C). These results suggested that FGF-21 inhibited the expression of inflammatory cytokines and collagen genes in pulmonary fibrosis cell models.

Discussion

Pulmonary fibrosis is a common stage of many chronic lung disease and the main pathological basis of respiratory failure. It is characterized by inflammatory cell infiltration, fibrous hyperplasia, ECM reconstruction, and excessive deposition, eventually leading to the destruction of lung architecture and dysfunction (Tao et al. 2021). Recent years, the incidence of pulmonary fibrosis has been increasing and is more common in the elderly. The disease has a median survival of only 3 to 5 years, and the 5-year survival rate is less than 30% which is called "the cancer that's not cancer" (Raghu et al. 2006). Pirfenidone exerted anti-inflammatory and anti-oxidative activities and had the therapeutic effect on multiple organ fibrosis including liver fibrosis, myocardial fibrosis, renal fibrosis, and pulmonary fibrosis (Cao et al. 2022; Aimo et al. 2020; Cho and Kopp 2010; Rockey 2008). However, FGF-21 had also important effects on anti-oxidative and anti-inflammatory and attenuated liver fibrosis. Therefore, we proposed that FGF-21 had the possibility to treat pulmonary fibrosis; then, the preventive and therapeutic effects of FGF-21 were verified in pulmonary fibrosis both in vivo and vitro.

Despite some limitations with regard to recapitulation of human disease, currently, the BLM-induced lung injury is the best model used to investigate potential pathways involved in the pathogenesis of pulmonary fibrosis and to explore therapeutic approaches (Kolb et al. 2020). As is reported, BLM-induced lung injury in mice involves two phases, including the early inflammatory response stage and later pulmonary fibrosis stage (Wilson and Wynn 2009), which is evident at 14 days and follows maximal responses between 21 and 28 days. The results under light microscope showed that there were a large number of inflammatory cell infiltration and fibroblast hyperplasia at 14 days and significant honeycomb lung structures at 21 days in BLM-induced pulmonary fibrosis, which indicated that fibrosis had developed. After the pretreatment of FGF-21, the degree of inflammation significantly reduced at 14 days, and alveolar morphology begun to recover at 28 days with the dose increased; in addition, recovery of mice in the treatment group was equally significant and even better than those in the prevention groups, suggesting that FGF-21 has a protective and therapy effect on BLM-induced pulmonary fibrosis in mice.

During the early stages of pulmonary fibrosis, macrophages serve as a central contributor to this process via the production of cytokines such as TNF-α, IL-8, and TGF-β, creating a fibrotic microenvironment and inducing the accumulation of ECM (Frangogiannis 2020). The high expression of these inflammatory factors are the characteristics in the formation of pulmonary fibrosis; thereby, the expression of TNF-α, IL-8, and TGF-β was determined in the lung tissue in mice. The result indicated that FGF-21 decreased the expression of these inflammatory mediators by BLM-induced and ultimately alleviated pulmonary fibrosis. Among these fibrogenic factors, TGF-β is the most pivotal profibrotic molecule. Several studies show that TGF-β has long been regarded as a

central mediator of tissue fibrosis that involves multiple organs including the skin, liver, kidney, and lung. And TGF-β also plays an important role in the development or progression of pulmonary fibrosis, which involved multiple stages of fibrosis, such as the secretion of extracellular matrix and inflammatory cytokines and the differentiation of fibroblasts (Adam et al. 2000). Differentiation of lung fibroblasts to myofibroblasts induced is a key event in the pathogenesis of pulmonary fibrosis, which are characterized by a-SMA expression and increased generation and secretion of ECM proteins, including collagen I and collagen III, which then aggravate the development of pulmonary fibrosis (Frangogiannis 2020). Both in gene and protein levels, the results clearly demonstrated that FGF21 treatment reduced the TGF-β expression level in vivo and in vitro. As well as the myofibroblast-associated gene α-SMA, the results distinctly indicated that FGF-21 injection was able to inhibit the α-SMA expression around the trachea, which was a hallmark of myofibroblast differentiation. The results indicated that the inhibitory effects of FGF-21 on pulmonary fibrosis might relate to prevent the fibroblast differentiation. After fibroblasts differentiate into myofibroblasts, myofibroblasts secrete a large amount of ECM which mostly constitute of collagen I and collagen III. HYP is considered as an important component of collagen reaction. The level of HYP in the lung tissue of mice decreased appreciably through FGF-21 intervention. In addition, the expression of α-SMA, collagen I, and collagen III showed the consistent results. These results confirmed the anti-fibrosis effect of FGF-21 once again.

In this study, an in vitro model of pulmonary profibrosis was established by BLM in THP-1 macrophages and evaluated the effects of FGF-21 on pulmonary fibrosis containing the inflammation and collagen accumulation. THP-1 macrophages as macrophage was often used to the model of inflammation (Kollarova et al. 2018); however, inflammation and collagen accumulation were found in BLM-induced THP-1 macrophages. BLM stimulated differentiated THP-1 cells to secrete inflammatory factors and collagen which reached peak at 24 and 48 h after molding. These results demonstrated that the THP-1 macrophages were useful as a model for the study of pulmonary fibrosis which was composed of inflammatory response in the early stage and collagen accumulation in the late stage. At the same time, FGF-21 reduced the mRNA and protein expression levels of TGF-β and α-SMA in THP-1 macrophages. The mRNA expression levels of IL-8, TNF-α, Col-1, and Col-3 decreased gradually as the dose of FGF-21 increased in vitro models. In conclusion, this study demonstrated that FGF-21 could antagonize the BLM-induced, macrophage-mediated pulmonary fibrosis.

Conclusion

In summary, FGF-21 effectively alleviated BLM-induced pulmonary fibrosis in mouse and cell models. FGF-21 inhibited the expression TGF-β and α-SMA, inhibited the prophase inflammatory response and anaphase ECM deposition, and in turn, inhibited the occurrence and development of pulmonary fibrosis. Therefore, FGF-21 had both preventive and therapeutic effects on BLM-induced pulmonary fibrosis by inhibiting inflammatory response and collagen synthesis in vitro and in vivo. In addition, FGF-21 may be a candidate for further drug development for treatment of pulmonary fibrosis.

Data availability All data generated or analyzed during this study are included in this article.

Code availability Not applicable.

Declarations

Competing interests The authors declare no competing interests.

Consent to participate Not applicable.

Consent for publication Not applicable.

Conflict of interest The authors declare no competing interests.

References

Adam PJ, Regan CP, Hautmann MB, Owens GK (2000) Positive- and negative-acting Kruppel-like transcription factors bind a transforming growth factor beta control element required for expression of the smooth muscle cell differentiation marker SM22alpha in vivo. J Biol Chem 275:37798–37806

Aimo A, Cerbai E, Bartolucci G, Adamo L, Emdin M (2020) Pirfenidone is a cardioprotective drug: Mechanisms of action and preclinical evidence. Pharmacol Res 155:104694

Ashcroft T, Simpson JM, Timbrell V (1988) Simple method of estimating severity of pulmonary fibrosis on a numerical scale. J Clin Pathol 41:467–470

Cao ZJ, Liu Y, Zhang Z, Yang PR, Li ZG, Song MY, Qi XM, Han ZF, Pang JL, Li BC, Zhang XR, Dai HP, Wang J, Wang C (2022) Pirfenidone ameliorates silica-induced lung inflammation and fibrosis in mice by inhibiting the secretion of interleukin-17A. Acta Pharmacol Sin 43:908–918

Cho ME, Kopp JB (2010) Pirfenidone: an anti-fibrotic therapy for progressive kidney disease. Expert Opin Investig Drugs 19:275–283

Frangogiannis N (2020) Transforming growth factor-β in tissue fibrosis. J Exp Med 217:e20190103

Goodwin A, Jenkins G (2009) Role of integrin-mediated TGFbeta activation in the pathogenesis of pulmonary fibrosis. Biochem Soc Trans 37:849–854

Kalluri M, Luppi F, Ferrara G (2020) What patients with idiopathic pulmonary fibrosis and caregivers want: filling the gaps with patient reported outcomes and experience measures. Am J Med 133:281–289

Kang H (2017) Role of microRNAs in TGF-β signaling pathway-mediated pulmonary fibrosis. Int J Mol Sci 18:2527

Kolb P, Upagupta C, Vierhout M, Ayaub E, Kolb MRJ (2020) The importance of interventional timing in the BLM model of pulmonary fibrosis. Eur Respir J 55:1901105

Kollarova J, Cenk E, Schmutz C, Marko D (2018) The mycotoxin alternariol suppresses lipopolysaccharide-induced inflammation in THP-1 derived macrophages targeting the NF-κB signalling pathway. Arch Toxicol 92:3347–3358

Kseibati MO, Sharawy MH, Salem HA (2020) Chrysin mitigates BLM-induced pulmonary fibrosis in rats through regulating inflammation, oxidative stress, and hypoxia. Int Immunopharmacol 89:107011

Li S, Guo XC, Zhang T, Wang N, Li JY, Xu PF, Zhang SQ, Ren GP, Li DS (2017) Fibroblast growth factor 21 ameliorates high glucose-induced fibrogenesis in mesangial cells through inhibiting STAT5 signaling pathway. Biomed Pharmacother 93:695–704

Phan THG, Paliogiannis P, Nasrallah GK, Giordo R, Pintus G (2021) Emerging cellular and molecular determinants of idiopathic pulmonary fibrosis. Cell Mol Life Sci 78:2031–2057

Pourgholamhossein F, Rasooli R, Pournamdari M, Pourgholi L, Samareh-Fekri M, Ghazi-Khansari M, Iranpour M, Poursalehi HR, Heidari MR, Mandegary A (2018) Pirfenidone protects against paraquat-induced lung injury and fibrosis in mice by modulation of inflammation, oxidative stress, and gene expression. Food Chem Toxicol 112:39–46

Raghu G, Weycker D, Edelsberg J, Bradford WZ, Oster G (2006) Incidence and prevalence of idiopathic pulmonary fibrosis. Am J Repspir Crit Care Med 174:810–816

Rockey DC (2008) Current and future anti-fibrotic therapies for chronic liver disease. Clin Liver Dis 12:939–962

Tao LJ, Cao J, Wei WC, Xie HF, Zhang M, Zhang CF (2017) Protective role of rhapontin in experimental pulmonary fibrosis in vitro and in vivo. Int Immunopharmacol 47:38–46

Tao NN, Li K, Liu JJ, Fan GQ, Sun TY (2021) Liproxstatin-1 alleviates BLM-induced alveolar epithelial cells injury and mice pulmonary fibrosis via attenuating inflammation, reshaping redox equilibrium, and suppressing ROS/p53/α-SMA pathway. Biochem Bioph Res Co 551:133–139

Wilson MS, Wynn TA (2009) Pulmonary fibrosis: pathogenesis, etiology and regulation. Mucosal Immunol 2:103–121

Xie T, Leung PS (2017) Fibroblast growth factor 21: a regulator of metabolic disease and health span. Am J Physiol Endocrinol Metab 313:E292–E302

Xu PF, Zhang YJ, Liu YY, Yuan QY, Song LY, Liu MY, Liu ZH, Yang YB, Li JY, Li DS, Ren GP (2016) Fibroblast growth factor 21 attenuates hepatic fibrogenesis through TGF-beta/smad2/3 and NF-kappa B signaling pathways. Toxicol Appl Pharm 290:43–53

Yang QF, Zhang P, Liu T, Zhang X, Pan XC, Cen YY, Liu Y, Zhang HG, Chen XH (2019) Magnesium isoglycyrrhizinate ameliorates radiation-induced pulmonary fibrosis by inhibiting fibroblast differentiation via the p38MAPK/Akt/Nox4 pathway. Biomed Pharmacother 115:108955

Zhang YK, Lu P, Qin H, Zhang YL, Sun XR, Song XN, Liu JJ, Peng H, Liu YT, Nwafor EO, Li JW, Liu ZD (2021) Traditional Chinese medicine combined with pulmonary drug delivery system and idiopathic pulmonary fibrosis: rationale and therapeutic potential. Biomed Pharmacother 133:111072